Freezing, melting and the glass transition in a suspension of hard spheres

2002 J. Phys.: Condens. Matter 14 7699

(http://iopscience.iop.org/0953-8984/14/33/310)

INSTITUTE OF PHYSICS PUBLISHING JOURNAL OF PHYSICS: CONDENSED MATTER

J. Phys.: Condens. Matter **14** (2002) 7699–7717 PII: S0953-8984(02)38826-X

Freezing, melting and the glass transition in a suspension of hard spheres

W van Megen

Department of Applied Physics, Royal Melbourne Institute of Technology, Melbourne, Victoria 3000, Australia

Received 1 July 2002
Published 9 August 2002
Online at stacks.iop.org/JPhysCM/14/7699

Abstract

When a suspension of hard spheres traverses the freezing volume fraction we find discontinuous changes in the character of the tagged particle density. In particular, the velocity auto-correlation function develops a negative algebraic decay and the fluctuations become subject to interruption. From these, and the exponent of the algebraic growth of the non-Gaussian parameter, the difference in mode of relaxation of the density fluctuations between the stable and metastable colloidal fluids can be quantified. A diagrammatic scheme is proposed that reconciles the dynamics of phase transitions observed in hard-sphere colloids.

1. Introduction

It is quite some years ago on a convivial evening that Peter Pusey, in the presence of his family and myself, announced that they were in the company of two people whose combined knowledge about Brownian motion was greater than that of any other duo. A curious comment since, at the time, I understood next to nothing about the subject. However, over the subsequent years during which Peter and I collaborated, I learnt a great deal from him about Brownian motion and how to measure it by means of dynamic light scattering. It is my privilege, therefore, to report some results of light scattering experiments that Peter once suggested to me and to discuss these in relation to a few particular aspects of his past work.

The first of these is one in which he, in collaboration with George Paul [1], presented the first statistically significant experimental verification of the so-called 'hydrodynamic tail'. This refers to the algebraic decay of the velocity auto-correlation function (VAF) of a molecule in a liquid, or a particle suspended in it, due to the enhancement of its instantaneous velocity by the feedback of the liquid's rotational momentum current [2]. Hydrodynamic theory [3] shows that the VAF is positive and decays as the power law $\tau^{-3/2}$. By carefully analysing the displacement statistics of particles in a very dilute suspension, the experiment of Pusey and Paul reveals a small but systematic, timescale-invariant deviation from normal diffusion consistent with the predicted non-steady motion, to delay times of 10^{-3} s.

0953-8984/02/337699+19$30.00

Considerations of the dynamical properties of suspensions are generally predicated on the assumption that random thermal fluctuations in the suspending liquid, which propel the particles, are dissipated by steady flow [4]. In other words, it is presumed that, over time intervals where significant movement of the suspended particles is evident, the liquid is in equilibrium. The question is whether, in view of what hydrodynamics dictates, this presumption is valid even as a first-order approximation when the particulate phase is not in equilibrium, i.e., when the volume fraction of the suspension exceeds the freezing value.

This brings me to the second component of Peter's work, that concerned with the order–disorder, or freezing–melting, transition in suspensions of hard spheres [4]. The present view of the mechanism by which this transition occurs is, like the formation of a raindrop, based on the classical idea of nucleation and growth [5]. This view holds that by a fortuitous but random sequence of movements, particles assemble into clusters. Clusters big enough that the thermodynamic bulk and surface forces are balanced form (stable) nuclei on which growth takes place. Inquiry into the mechanism of the transition has been largely focused on the change in structure and influenced by the classical view. The spectacular contrast between an amorphous colloidal fluid and the opalescent crystal [6] may also tend to direct focus exclusively onto the structural difference between these phases.

The gross macroscopic difference between a fluid and a crystal is that the latter supports a shear stress while the former does not. The crystal yields along cleavage planes once the applied stress exceeds a certain value. A colloidal crystal quivers when tapped. This must be gentle, for vigorous treatment shear melts the crystal. From this perspective, one might pose the following questions: How do planes, or even lines, of particles come into existence during crystallization? At what stage of this process does the system develop the capacity to support phonons?

A third aspect of Peter's work deals with polydispersity, its measurement [7] and its influence on the phase behaviour [4]. It appears that the hard-sphere-like polymer particles that we have used in many of our experiments have, by some stroke of good fortune, just the right degree of polydispersity. The latter, typically around 5%, causes very significant delay in the formation of Bragg reflecting crystals but has comparatively little effect on the equilibrium phase behaviour or the fluctuations [8]. So, this fortuitous degree of polydispersity still allows one to state, fairly precisely, the volume fraction where the colloidal fluid crosses over from one that is thermodynamically stable to one that is metastable, while it also causes the metastable fluid to maintain its integrity long enough for one to study its fluctuations.

Numerous dynamic light scattering experiments, performed in Malvern [9], Edinburgh [10] and Melbourne [11], have studied the number density fluctuations in these suspensions. They show that, as the volume fraction is increased, the decay of the fluctuation auto-correlation function becomes slower, deviates more and more from exponential and develops a two-stepped decline to the noise floor. The glass transition (GT) is located at the volume fraction where the second step is arrested. However, there appears to be no discontinuity or qualitative change in the correlation function when the freezing volume fraction is traversed. This lack of an obvious change gives the impression that there is no fundamental difference between the fluctuations in stable and metastable fluids, and lends support to the view, proposed by mode-coupling theory [12], that the GT is purely dynamical in origin. It also supports the idea that nucleation of the crystal phase is entirely accidental. We must wonder, nonetheless, whether we have missed something.

The experiments to which I referred in the opening paragraph measure the self-intermediate-scattering function (ISF), the correlation function of tagged particle density fluctuations, in a suspension of hard spheres. The analysis of the data employs various schemes to separate the fast and slow components of the fluctuations. Our purpose is twofold; firstly, to

expose aspects of the fluctuations that change their character as the freezing volume fraction is traversed and, secondly, to see whether all aspects of the fluctuation are consistent with the assumption that thermal fluctuations are dissipated by steady motion.

2. Self-intermediate-scattering function

The quantity of interest is the self-ISF

$$F(q,\tau) = \langle \exp[\mathrm{i}\boldsymbol{q}\cdot\Delta\boldsymbol{r}(\tau)]\rangle. \tag{1}$$

Here $\boldsymbol{q}$ is the wavevector and $\Delta\boldsymbol{r}(\tau)$ is the particle displacement in the time interval τ. The angular brackets denote the average over an ensemble. The right-hand side of equation (1) is then rotationally invariant and the cumulative function, $\ln F(q,\tau)$, can be expanded as follows [13]:

$$\ln F(q,\tau) = -\langle\Delta r^2(\tau)\rangle\frac{q^2}{6} + \frac{1}{2}\alpha(\tau)\left(\frac{q^2}{6}\right)^2 + \cdots. \tag{2}$$

The successive cumulants $\langle\Delta r^2(\tau)\rangle$ and

$$\alpha(\tau) = \tfrac{3}{5}\langle\Delta r^4(\tau)\rangle - \langle\Delta r^2(\tau)\rangle^2, \tag{3}$$

respectively, represent the mean squared displacement (MSD) and the first deviation of the particle displacement distribution from Gaussian.

Details of the experimental method are described elsewhere [14]. However, it must be mentioned here that, over the range of wavevectors $1.3 \leqslant qR \leqslant 3.8$, $F(q,\tau)$ showed no systematic deviations from the expansion in equation (2) to quadratic order in q^2.

It is evident from the definition, equation (1), that the self-ISF measures the ensemble average of fluctuations in the scattered light field resulting from sequences of phase-preserving steps in the direction of the vector $\boldsymbol{q}$. So long as such sequences occur with random probability the ISF decays exponentially:

$$F_0(q,\tau) = \exp[-Dq^2\tau]. \tag{4}$$

Here the diffusion coefficient, D, characterizes the linear growth of the MSD due to entirely random steps; $\langle\Delta r^2(\tau)\rangle = (6)D\tau$. Any aspect of the fluctuations that deviates from equation (4) will be referred to as 'systematic'.

It follows from equation (2) that the Gaussian self-ISF

$$F^{(G)}(q,\tau) = \exp[-\langle\Delta r^2(\tau)\rangle q^2/6], \tag{5}$$

is recovered in the limit of infinite spatial integration ($q \to 0$), irrespective of the suspension concentration.

The VAF,

$$Z(\tau) = \frac{\mathrm{d}^2}{\mathrm{d}\tau^2}\langle\Delta r^2(\tau)\rangle, \tag{6}$$

exposes any systematic movement superposed on random movement.

3. Microscopic perspectives

Before discussing the experimental results we turn to several molecular dynamics studies. These give a microscopic view of how systematic movement comes into existence. They may also provide a clue about how one might identify such movement spectroscopically.

Molecular dynamics simulations by Rahman [15] showed that the displacement of an atom in a liquid is favourably directed towards the elongation of its first coordination shell. They also show that this correlation, between the magnitude and direction of an atom's displacement, gives rise to a negative and monotonically decaying velocity correlation which persists considerably longer than the collision-induced back-scatter. As such, this tendency of the movement of particles to be confined to one dimension is independent of the microscopic dynamics, be they ballistic or diffusive.

A picture emerging from this is that an atom exploits the larger-than-average gap created by the movements of its neighbours. The gap that the atom leaves behind it can then be exploited by another atom, and so forth. So as the observation interval increases, encompassing an increasing number of collisions or moves by the atoms, a file or queue of atoms moving in concert becomes evident. Numerous more recent microscopic studies show directly this sort of cooperation among particles in a dense fluid [16].

The ultimate inference Rahman made from his computations was that anharmonic rattling of particles in one momentarily well-defined plane creates the gaps that allow 'slip' in the direction perpendicular to this plane. In other words, an impediment to the decay of the local or microscopic longitudinal particle current by (anharmonic) packing constraints creates a transverse current. This local symmetry breaking manifests itself by a slowly and monotonically decaying negative VAF.

The molecular dynamics studies of Alder and Wainwright [2] show that the oblique component of the momentum transfer gives, after many collisions, a positive feedback to an atom's velocity. This effect of the finite size of atoms is manifested in the continuum by the double vorticity in the Navier–Stokes equation.

The computer experiments of Alder and Wainwright and Rahman respectively demonstrate the microscopic origins of positive and negative sources of feedback on a particle's movement. Both are consequences of packing constraints and they both act to maintain the direction of a particle's velocity. This indicates ubiquity of movement in files and that these files may have a purpose.

In a fluid where the atomic collisions are instantaneous, the two feedback mechanisms may have comparable timescales and delaying influences. However, in a suspension one anticipates that the negative feedback to a particle's movement due to the direct effect of packing constraints of its neighbours will be delayed relative to the positive feedback of the vorticity that the particle creates in the suspending liquid.

4. Results and spectroscopic perspectives

A detailed account of the measurements of the self-ISF will be presented elsewhere [17]. Only an abridged version of the results appropriate to the issues raised in section 1 is shown here. The freezing, melting and GT volume fractions of the hard-sphere suspension considered here are $\phi_f = 0.494$, $\phi_m = 0.54 \pm 0.005$ and $\phi_g = 0.575 \pm 0.005$, respectively [6]. Thus, the volume fraction ϕ_f delineates colloidal fluids in stable and metastable equilibrium.

In the results below, all distances are expressed in units of the particle radius, R (=200 nm), and delay times in units of the Brownian characteristic time, $\tau_b = R^2/(6D_0)$ (=0.021 s), where D_0 is the diffusion coefficient of an isolated sphere.

Figure 1 shows typical results for the ISF measured at the wavevector given by $qR = 1.3$. This value of qR should be read relative to the position, $qR \approx 3.5$, of the primary maximum in the static structure factor. Of course, as explained in previous work [14], scattering from the structure is suppressed, so only the tagged particle density fluctuations are measured. By fitting the quantity $\exp(-D_s q^2 \tau)$ to the initial decay of $F(q, \tau)$, one determines the short-

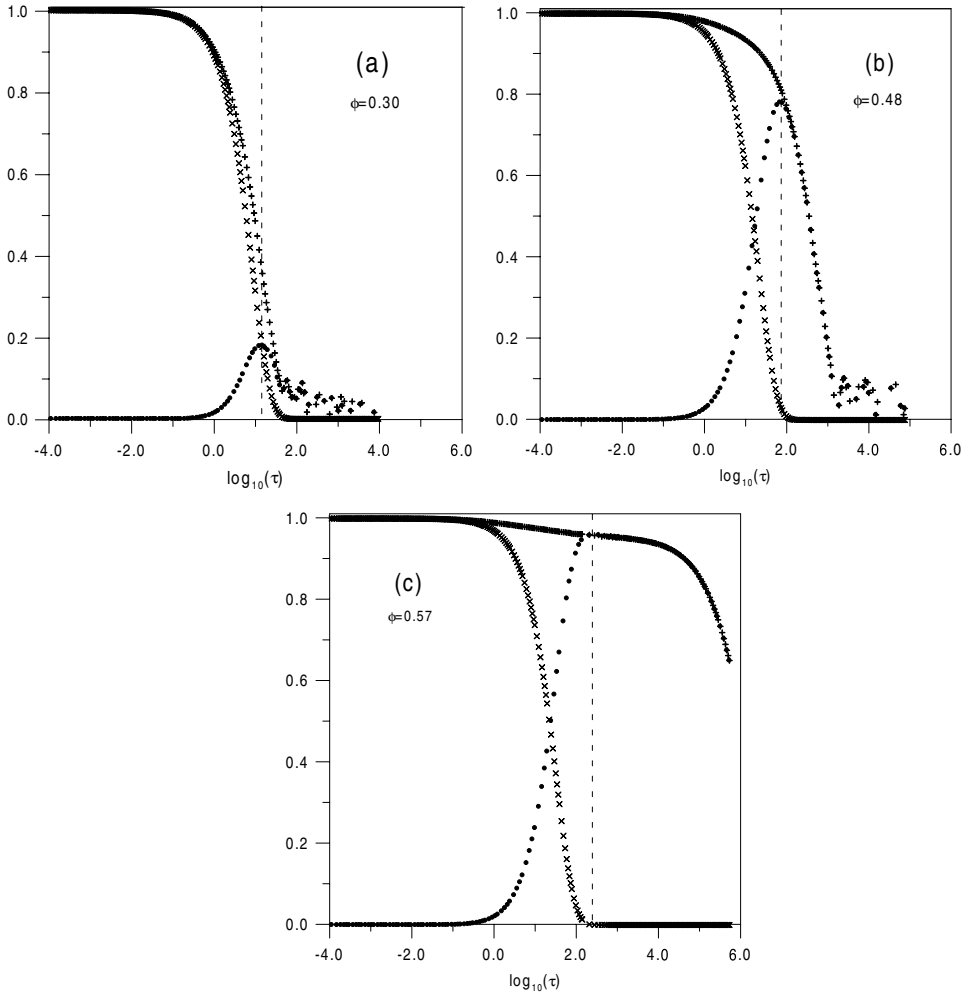

Figure 1. Self-ISF, $F(q,\tau)$ (+ signs); the component of the ISF, $\exp[-D_s q^2\tau]$, due to random fluctuations (crosses); systematic component, $T(q,\tau) = F(q,\tau) - \exp[-D_s q^2\tau]$ (dots); (a) $\phi = 0.30$, (b) $\phi = 0.48$, (c) 0.57. The dashed vertical line passes through the maximum in $T(q,\tau)$.

time self-diffusion coefficient, D_s [14]. The latter characterizes the component of the thermal fluctuations dissipated by steady motion. D_s decreases by approximately a factor of 10 when the volume fraction is increased from zero to about 0.5. In the results, discussed below, we identify several crossover times that are independent of ϕ. Thus, we will encounter aspects of the dynamics that cannot be reconciled in terms of steady dissipation of thermal fluctuations.

For now we consider the difference

$$T(q,\tau) = F(q,\tau) - \exp(-D_s q^2\tau) \tag{7}$$

also shown in figure 1. This quantity filters out the effect of the random fluctuations and exposes a slower mode of coherent fluctuations. We refer to this slower, non-random mode as 'systematic' and the objective here is to identify its statistical properties. The main feature to note is that, for the lowest volume fraction ($\phi = 0.30$, figure 1(a)), random fluctuations

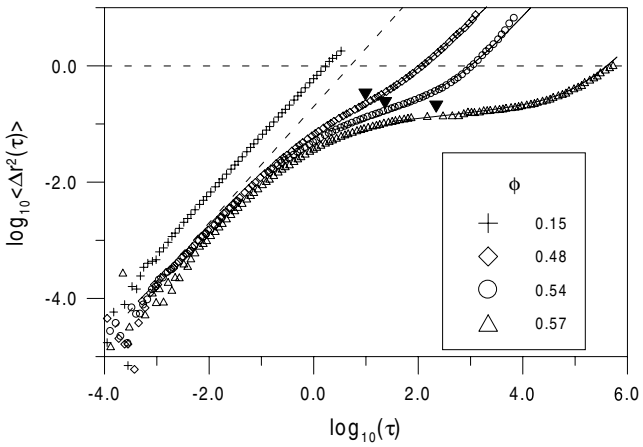

Figure 2. Logarithm of the MSD versus logarithm of delay time at the volume fractions indicated. The arrow points to the inflection (at τ_m) in each curve. The solid curves are fits of the function defined in equation (9) to the data. The dashed line is a line of unit slope.

stimulate and continue to be available to dissipate the systematic mode, $T(q, \tau)$. This overlap of random and systematic fluctuations occur as long as $\phi < 0.48$. Once this volume fraction is exceeded, random fluctuations are integrated to the noise floor over the interval where $T(q, \tau)$ attains its maximum. It is apparent, from figure 1(c), that the fully developed systematic mode then waits before it decays. These results suggest a change at $\phi = 0.48$, i.e., around ϕ_f, in the process of coarse-graining of the systematic mode.

It must be pointed out that the experimental results are based on ensemble averages of the phases, $\boldsymbol{q} \cdot \Delta \boldsymbol{r}$, in equation (1). Thus, we can draw statistically significant inferences about the density fluctuations although their statistics are generally not normal.

Typical results on the MSD are shown in figure 2. The double-logarithm representation exposes those regions where normal linear diffusion obtains by lines of unit slope, i.e., $\langle \Delta r^2(\tau) \rangle \propto \tau$. An arrow points to the delay time, τ_m, where a curve in figure 2 has an inflection, i.e., where the systematic mode has its strongest projection on, and incurs the greatest delay in, the growth of the second moment of the tagged particle density fluctuations. The root mean squared (RMS) distance, R_m, is defined by $\langle \Delta r^2(\tau_m) \rangle = R_m^2$.

The quantities R_m and τ_m are shown in figure 3 in terms of ϕ. One sees that R_m decreases linearly with ϕ up to 0.48 and then exhibits no further systematic change. Contrasting with this, τ_m is independent of ϕ up to 0.52 and then increases sharply. Within the resolution of the volume fraction of the samples in these experiments, the results for R_m suggest a structural change in the systematic mode at the freezing volume fraction, ϕ_f; once this volume fraction is exceeded the systematic mode submits to no further compression. The result for τ_m hints at a change in dynamics at the melting volume fraction, ϕ_m.

Another quantity that we consider is the slope of the tangent to the point (R_m, τ_m) on each of the curves in figure 2:

$$\nu = \left[\frac{\mathrm{d} \log \langle \Delta r^2(\tau) \rangle}{\mathrm{d} \log(\tau)} \right]_{\tau = \tau_m}. \tag{8}$$

Note, from figure 4, that ν passes through the value $1/2$ around ϕ_f and converges to zero at the GT.

In the index ν we read the statistical manifestation of the tendency, exposed in Rahman's computations, of particles to cooperate by moving in queues. This assertion is based on the fact

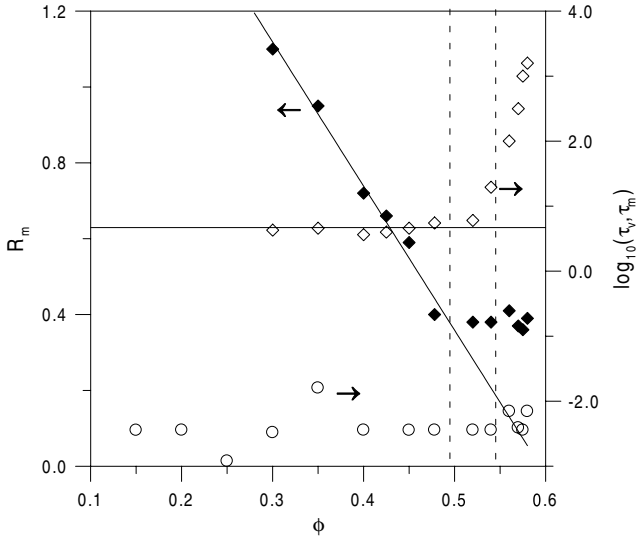

Figure 3. Delay times τ_v (circles), where the VAF has its minimum, and τ_m (open diamonds), where the MSD (figure 2) has the inflection. Delay times are given by the right-hand axis. The MSD $\langle \Delta r^2(\tau_m) \rangle = R_m^2$ (filled diamonds). The dashed vertical lines are drawn at the freezing and melting volume fractions. The continuous lines are drawn as a guide.

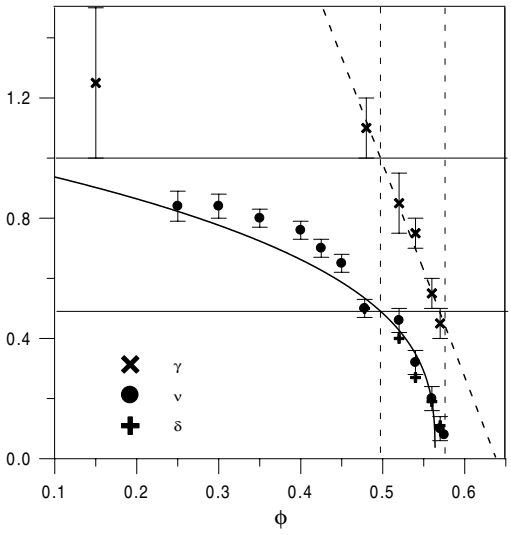

Figure 4. The index ν, defined in equation (8). The exponent δ of the systematic mode—the first term in equation (9). The index γ of the non-Gaussian parameter. The continuous curve is the function given by equation (21) and the dashed line is the line of best fit through the index γ. The dashed vertical lines are drawn at $\phi = \phi_f$ and $\phi = \phi_g$. See the text for details.

that the MSD of particles in single file increases in proportion to the square root of the delay time [18]. This asymptotic result, recently confirmed experimentally [19], obtains after the contribution from random movement of the particles has decayed to the noise floor. Thus, the only movement that survives coarse-graining to τ_m at volume fractions exceeding the freezing value is coherent movement in one dimension.

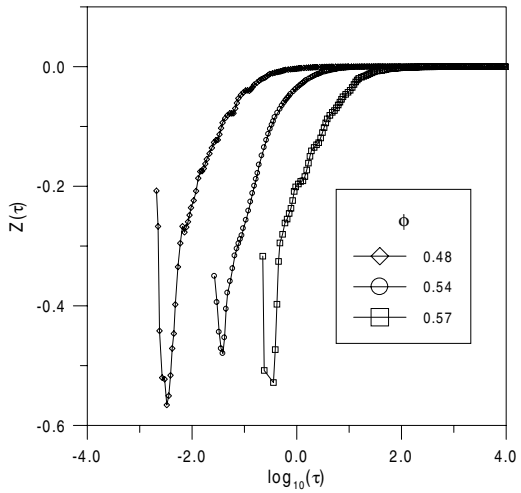

Figure 5. The VAF, $Z(\tau)$, at the volume fractions indicated. For clarity, each successive data set has been translated along the log τ axis by two.

It is also well known that the metastable fluid distinguishes itself structurally, from the stable fluid, by a narrow peak in the radial distribution function that corresponds to the contact limit of three (or more) collinear spheres [20]. In consideration of this and the observation that R_m is independent of ϕ (for $\phi > \phi_f$) we infer that in the metastable fluid the systematic mode comprises a linear queue of three (or more) particles in contact.

The VAFs, $Z(\tau)$, are shown in figure 5. The initial decrease in these, just discernible from the noise, indicates that memory of the particle's (initial) velocity, or momentum, persists until, at τ_v, it is overwhelmed by the effects of interactions with its neighbours. For a completely isolated particle in the liquid we would expect, in accordance with the experiment of Pusey and Paul [1] and the prediction of hydrodynamics [3], $Z(\tau)$ to remain positive and decay as $\tau^{-3/2}$. At finite volume fraction, velocity reversals caused by packing constraints press down on the influence of this non-steady movement. This results in the more slowly decaying negative VAF which, according to our interpretation of Rahman's computations in section 3, is the manifestation of the transverse mode.

There is no indication, in figure 5, that the velocities are uncorrelated. In fact, the position of the minimum of the VAF, at τ_v ($\approx 10^{-2}$), is approximately four orders of magnitude larger than the characteristic decay interval based on the assumption that thermally stimulated particle movement is dissipated by steady flow [4]. It appears, therefore, that the effect of vorticity or non-steady flow cannot be ignored. Moreover, as indicated in figure 3, this effect starts to couple to systematic velocity reversals over an interval, τ_v, that shows no systematic variation with ϕ. It also appears that this coupling is maintained until, at τ_m, the cooperative consequences of velocity reversals are fully manifested. From figure 3 one can determine that the delay, τ_m/τ_v, between the crossover times, τ_m and τ_v, is approximately three decades and independent of ϕ below ϕ_m. This transmission delay increases sharply when ϕ exceeds ϕ_m.

The above inference has two consequences. First, there is no transmission delay between velocity reversals and the emergence of cooperation among the particles, i.e., $\tau_v = \tau_m$, when there is no suspending liquid and collisions among the particles are instantaneous. Second, the positive feedback, due to the coupling between a particle's momentum and its displacement, enhances the efficiency relative to random with which configuration space is explored.

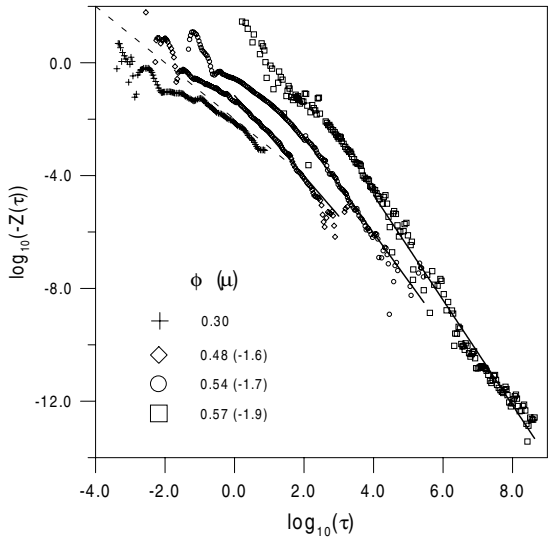

Figure 6. The VAF, expressed as $\log_{10}(-Z(\tau))$. Each successive data set has been translated along the $\log\tau$ axis by one. Volume fractions and the slope (μ) of the best-fitting straight line are indicated. The dashed line has slope -1.

Before confirming these consequences we continue consideration of the VAF. The present experiments extend over a considerably larger dynamical window than Rahman's computations. One sees from figure 5, and so much better in figure 6, how the local symmetry-breaking fluctuations, observed by Rahman, evolve over longer delay times.

For the higher volume fractions, $\phi \geqslant 0.48$, the results can be described by power laws, $Z(\tau) \sim -\tau^{-\mu}$, at long delay times. The best-fitting straight lines, from a lower limit of $\log(\tau) = 0$, give an index μ that increases from about 1.6 to about 2.0 as ϕ is increased towards ϕ_g. In view of the arbitrary lower limit and the noise on the data, there is considerable uncertainty in this exponent. However, identification of a power law in the VAF suggests that in addition to a normal diffusing term, linear in delay time, the MSD has a contribution proportional to τ^{δ}, where $\delta = -\mu + 2$. So, a possibly more accurate estimate of the index μ (or δ) is obtained by fitting the expression

$$\langle \Delta r^2(\tau \geqslant \tau_m)\rangle = \left[C\left(\frac{\tau}{\tau_m}\right)^{\delta} + \left(\frac{\tau}{\tau_m}\right)\right]\left(\frac{R_m^2}{C+1}\right), \tag{9}$$

to the measured MSD for $\tau \geqslant \tau_m$. This consistency check of the data uses the values of R_m and τ_m, shown in figure 3, and treats C and δ as free parameters. The fits are shown in figure 2. The index δ is shown in figure 4, and the parameter C in figure 7. From equations (8) and (9) one derives the relationship $\nu = (\delta C + 1)/(C + 1)$. The estimate of ν obtained here agrees with that obtained above directly from the MSD.

Given that $\delta < 1$, the diffusion coefficient obtained from equation (9) by taking the limit $\tau \to \infty$ is

$$D_l = \frac{R_m^2}{\tau_m(C+1)}. \tag{10}$$

The results of this estimate of the long-time self-diffusion coefficient are shown in figure 7.

This analysis suggests that in the metastable colloidal fluid the systematic mode, characterized by the amplitude C and exponent δ, maintains its integrity as an integral

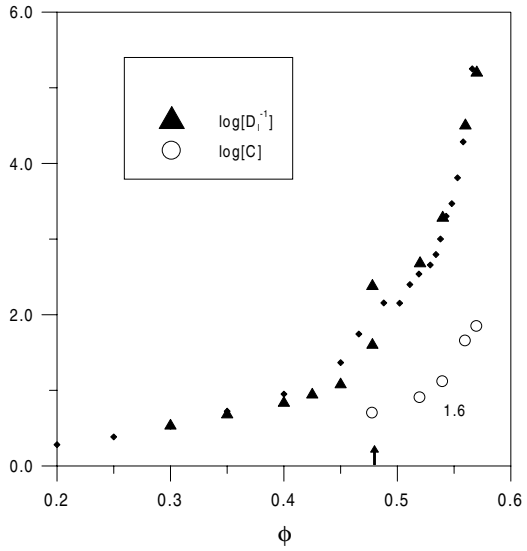

Figure 7. The logarithm of the coefficient C (circles), defined in equation (9). The logarithm of the inverse long-time diffusion coefficient D_l (triangles), given by equation (10) for $\phi \geqslant 0.48$ (to the right of the arrow) and equation (11) for $\phi < 0.48$ (to the left of the arrow). The small closed symbols correspond to values of D_l from [14].

component of the fluctuations to the upper limit of the experimental time window. By this we mean that movement of the systematic mode, or structural rearrangement of particles in a particular region, is non-random. The unavailability of random fluctuation to relax the systematic mode was also intimated from figure 1. This being the case, identification of a long-time diffusion coefficient implies the existence of statistically independent regions in the scattering volume. The coefficient, D_l, characterizes coarse-graining by averaging over these regions.

Increasing the duration of the measurement to the extent that the first term in equation (9) is negligible compared to the second may ultimately achieve an average over an ensemble of all possible displacements. However, such extension sees the onset of crystallization, i.e., the emergence of structures of size comparable to the scattering volume. Thus, eventual crystallization of the sample limits the time window over which fluctuations in the metastable fluid can be measured with statistical significance.

We now turn to volume fractions below 0.48. In these cases no power law is evident in the VAF (figure 6). However, we can still apply equation (9) by assuming that the systematic mode dissipates locally. This local equilibration, which by definition must occur in a stable fluid, can be invoked by allowing the index δ to approach unity from below. The diffusion coefficient obtained in this limit is

$$D_l = \frac{R_m^2}{\tau_m}. \tag{11}$$

The results for D_l obtained here are consistent with previous estimates obtained from the MSD at very long delay times (see figure 7).

Note that for the colloidal fluid in stable equilibrium the long-time diffusion coefficient is fully determined at τ_m and does not explicitly require the limit $\tau \to \infty$. Equations (10) and (11) indicate that D_l is determined by the mean squared amplitude, R_m^2, of the systematic movement of the particles and the delay, τ_m, of the non-steady response of the suspending

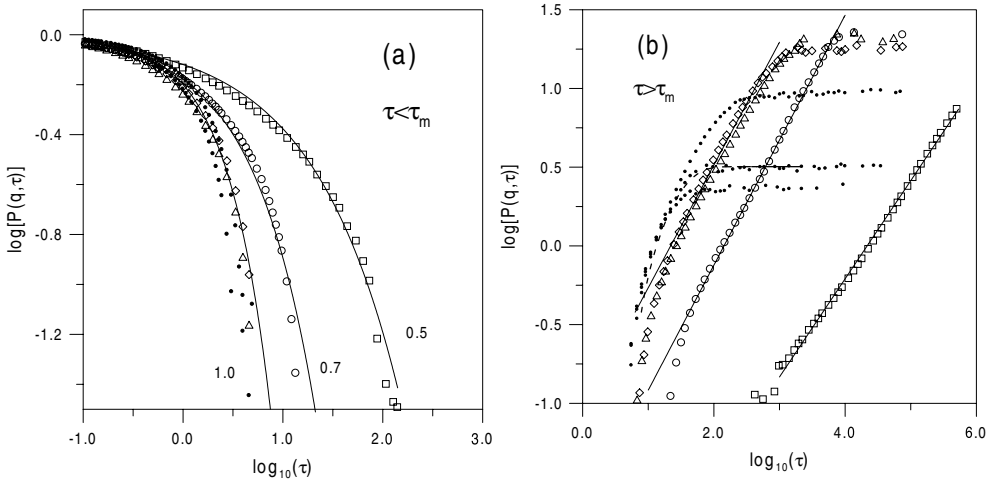

Figure 8. The logarithm of $P(q, \tau)$, defined in equation (13), for $\tau < \tau_m$ (figure 8(a)) and $\tau > \tau_m$ (figure 8(b)). Data are shown for volume fractions 0.48 (diamonds), 0.54 (circles), 0.57 (squares). The small closed symbols are results for lower ($\phi < 0.45$) volume fractions. The curves in figure 8(a) are given by equation (14) for the values of β indicated. In figure 8(b) the continuous lines are linear fits to the upper portions of the data and the broken curve corresponds to a single-exponential decay of the ISF.

liquid. The amplitude, C, of the systematic mode gives the metastable colloidal fluid an added impediment to diffusion.

Having shown that τ_m is the integration interval over which systematic movement is most strongly projected, we now use it to discriminate fast from slow fluctuations. The procedure has been employed in analysis of the (coherent) ISF by mode-coupling theory [21]. But, unlike the separation shown in figure 1, this procedure makes no assumption about the statistical properties of the fast fluctuations. From R_m, the amplitude

$$f(q) = F(q, \tau_m) = \exp[-q^2 R_m^2/6] \tag{12}$$

is calculated for the wavevector $qR = 1.3$. (As will be shown elsewhere [17], the Gaussian limit (equation (5)) is a good approximation of the self-ISF at this value of qR.) The quantity

$$P(q, \tau) = \left| \frac{F(q, \tau) - f(q)}{1 - f(q)} \right| \tag{13}$$

is shown in figure 8(a) for $\tau < \tau_m$ and figure 8(b) for $\tau > \tau_m$. Figure 8(a) indicates that, for ϕ up to 0.52, the results for $P(q, \tau < \tau_m)$ approximately coincide and they can be described by the exponential

$$P(q, \tau < \tau_m) \sim \exp[-b\tau^\beta], \tag{14}$$

with $b \approx 0.5$ and $\beta = 1$.

It was asserted above that memory of a particle's momentum is maintained for an interval that extends to τ_m. The exponential decay, seen in figure 8(a), implies that $P(q, \tau < \tau_m)$ captures the full ensemble of possible manifestations of this memory. Thus, for $\phi \leqslant 0.52$ memory of a particle's initial momentum is lost over the interval τ_m. This loss of momentum memory is consistent with the notion of a diffusing vorticity in the liquid [2]. We also see that, below approximately ϕ_m, τ_m and $P(q, \tau < \tau_m)$ are independent of ϕ. This suggests that the vorticity in the liquid couples to a structure that is common to all volume fractions below ϕ_m.

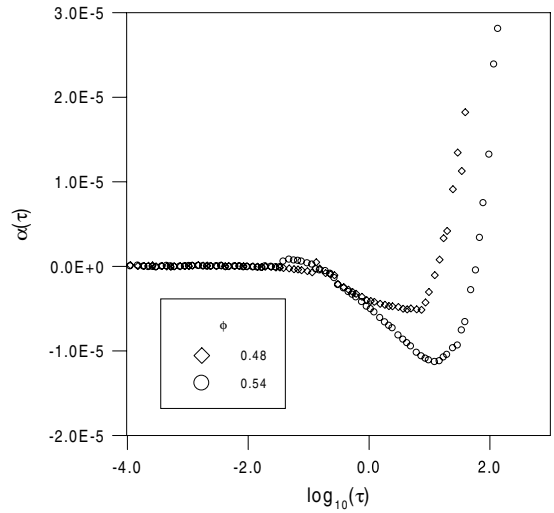

Figure 9. The non-Gaussian parameter, defined in equation (3), at the volume fractions indicated.

For larger ϕ, $P(q, \tau < \tau_m)$ becomes stretched; the parameter β in equation (14) required to describe the data decreases to $1/2$ as ϕ is increased towards ϕ_g. According to the above explanation, this implies that the vorticity couples to another structure whose relaxation time increases with ϕ. Moreover, the interval τ_m no longer captures all possible manifestations of this coupling. When ϕ is very close to ϕ_g, ambiguity in the estimate of R_m precludes estimation of β.

In figure 8(b) one observes that the decay, $P(q, \tau > \tau_m)$, of the slow fluctuations becomes exponential at long times for $\phi < 0.48$. We infer here that in stable equilibrium the slow fluctuations equilibrate because they see the fast fluctuations as random. However, for larger ϕ the slow decay maintains a power law

$$P(q, \tau > \tau_m) \sim \tau^{\lambda} \tag{15}$$

to the noise floor. Also, the index of the power law, $\lambda = 0.7 \pm 0.05$, shows no systematic variation with ϕ. Thus, there appears to be a universal source of (negative) feedback to a particle's movement in the metastable colloidal fluid. The power-law form of $P(q, \tau > \tau_m)$ also suggests that there is a contribution to the MSD, although possibly one that is latent, proportional to $\log(\tau)$.

The non-Gaussian parameter $\alpha(\tau)$, shown in figure 9, provides another perspective which lends support to some of the above inferences. The first of these derives from the location of the minimum in $\alpha(\tau)$ which, within experimental uncertainty, occurs at τ_m. Thus, for $\tau < \tau_m$, there is a monotonic increase in the efficiency, relative to random, with which particles explore configuration space. This confirms one of the consequences asserted above, that the positive feedback of the liquid's vorticity to the particle motion is maintained up to τ_m. It was also suggested that for ballistic hard spheres, $\tau_v = \tau_m$, resulting in a positive $\alpha(\tau)$ at all τ. Recent molecular dynamics studies of hard-sphere fluids confirm this to be the case [22].

The efficacy of the above feedback will be attenuated by a harmonic component in the interaction between the particles. Theory shows that the displacement statistics of a particle in a harmonic potential is Gaussian [23]. Therefore, the negative values of $\alpha(\tau)$ are also indicative of anharmonic confinement, as expected for hard-sphere particles. However, since the RMS displacement, R_m, is appreciably greater than the average gap between the particles, the simple concept of a particle confined by its instantaneous neighbours is not adequate.

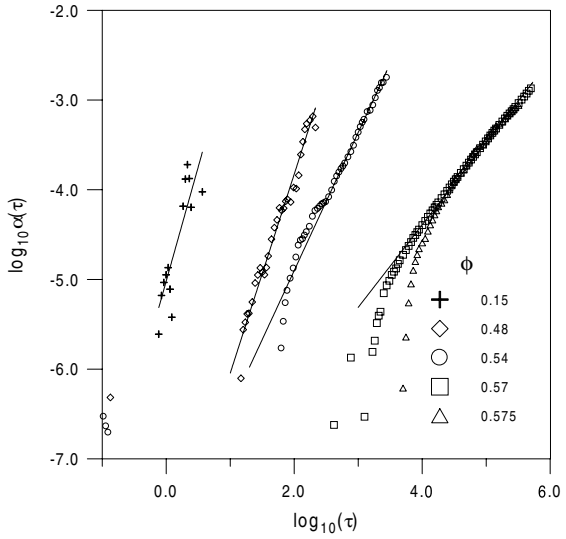

Figure 10. The logarithm of the non-Gaussian parameter at the volume fractions indicated. Best-fitting straight lines for the upper portions of the data are also shown. Half the value of the slope of each line is shown in figure 4.

Another interpretation of figure 9 can be given from the perspective of the particles, without explicit reference to the non-steady response of the liquid. Velocity reversals, evident for $\tau > \tau_v$, when imposed by purely reflecting (anharmonic) boundaries, increase the proportion of small displacements relative to that of a random distribution. This causes the term $\langle \Delta r^2(\tau) \rangle^2$ to increase faster than $\langle \Delta r^4(\tau) \rangle$, so $\alpha(\tau)$, defined in equation (3), initially decreases. With increasing delay time the cooperative consequences of these velocity reversals become increasingly evident. By 'cooperation' we mean that the proportion of large displacements is greater than normal, giving added weight to $\langle \Delta r^4(\tau) \rangle$ and causing $\alpha(\tau)$ to increase.

We now turn to the second aspect of the non-Gaussian parameter. In figure 10 one sees that at long delay times $\alpha(\tau)$ can be approximated by a power law, $G\tau^{2\gamma}$. The exponent γ is shown in figure 4.

This power-law behaviour may be explained as follows. First it is proposed, for the suspension in stable equilibrium ($\phi < \phi_f$), that for large τ both $\langle \Delta r^4(\tau) \rangle$ and $\langle \Delta r^2(\tau) \rangle^2$ increase in proportion to τ^2. The currently limited data are not incompatible with this. Cancellation of these moments to make $\alpha(\tau)$, defined in equation (3), vanish at all τ occurs only for an infinitely dilute suspension. At finite volume fraction, packing constraints lead to cooperation which, at large τ, results in a constant net lead of the fourth moment over (the square of) the second. The inference is that a divergence of $\alpha(\tau)$ in proportion to τ^2 indicates decay of the systematic mode by random fluctuations. This is consistent with the argument, based on the establishment of local equilibrium, that led to equation (11) for the long-time diffusion coefficient in the thermodynamically stable suspension. Despite the divergence of $\alpha(\tau)$, one sees from equation (2) that an exponentially decaying ISF is still recovered in the thermodynamic limit, for a suspension in stable equilibrium; limits are taken in the order $q \to 0$, $\tau \to \infty$, such that $q^2\tau \to 0$.

In the metastable suspension the exponent (2γ) of the power law that describes $\alpha(\tau)$ at large delay times is less than two. As argued already, equilibrium is not established locally in the metastable fluid and the only way of obtaining statistically significant results is by averaging over statistically independent regions in the scattering volume. The effect of this

apparent randomization can be superposed on the fluctuations by adding, to the second and fourth moments, terms that increase respectively with delay time as $D\tau$ and $E\tau^2$. That, for $\tau > \tau_m$, the MSD can be described by equation (9) confirms these suggestions in part. Further confirmation is obtained by rewriting equation (9) as

$$\langle \Delta r^2(\tau) \rangle = A\tau^\delta + D\tau, \tag{16}$$

and the fourth moment as

$$\langle \Delta r^4(\tau) \rangle = G\tau^{2\gamma} + E\tau^2. \tag{17}$$

Substitution of these expressions into equation (3) gives

$$\alpha(\tau) = \tfrac{5}{3}G\tau^{2\gamma} - A^2\tau^{2\delta} - 2AD\tau^{1+\delta} + (\tfrac{5}{3}E - D^2)\tau^2. \tag{18}$$

The coarse-graining or randomization introduced here, unlike that induced by random thermal fluctuations, is not subject to packing constraints and the concomitant imbalance of the second and fourth moments. Consequently, its contribution to the second and fourth moments must be balanced in a manner that nullifies the last term in equation (18). It has already been established, for the metastable suspension, that $\delta < \nu \leqslant 1/2$. Thus the emergence of a (positive) power law, of index $1 < 2\gamma < 2$, in $\alpha(\tau)$, is consistent with cancellation of the coefficients of τ^2 and the condition $2\gamma > 1 + \delta$. The results for the indices, shown in figure 4, comply with this condition. Conversely, the observation of a power-law increase of $\alpha(\tau)$ with index less than two indicates that the decay of the ISF is effected by averaging over independent localities in the scattering volume rather that by local randomization. This conclusion is consistent with that based on the MSD; in the metastable fluid one explicitly relies on averaging over independent regions because, locally, the systematic mode remains intact.

The line of best fit to γ versus ϕ (figure 4), through all except the lowest volume fraction for which $\alpha(\tau)$ has been measured, passes through the values $\gamma = 1$ and $1/2$ at $\phi_1 = 0.5 \pm 0.01$ and $\phi_2 = 0.575 \pm 0.005$. This line extrapolates to $\gamma = 0$ at $\phi_3 = 0.64 \pm 0.01$. The values of ϕ_1, ϕ_2 and ϕ_3 are consistent with the observed freezing, GT and random close-packing volume fractions.

Thus, at ϕ_g there appears to be another change of mechanism by which fluctuations decay. We return to the MSD for a closer inspection of this. We see from figure 7 that the long-time diffusion coefficient (equation (10)) converges to zero as ϕ approaches ϕ_g. Thus, at the GT, macroscopic diffusion stops. Figure 4 shows that the index δ, the power-law exponent of the systematic mode in equation (9), also converges to zero. However, the VAF still appears to maintain a power-law decay, $Z(\tau > 1) \sim \tau^{-2}$. One way to reconcile this form of the VAF and the approach of the exponent δ to zero, is for a contribution proportional to $\log(\tau)$ to emerge in the MSD. Thus, it appears that, as the GT is approached and both random and systematic movement arrest, the latent contribution, $\log(\tau)$, identified in figure 8(b), emerges. This also means that after the term proportional to $\tau^{2\gamma}$, in equation (18), the third term, now proportional to $\tau \log \tau$ and negative, is the next fastest. The emergence of the latter gives an explanation for the increasing curvature, seen (in figure 10) in the long-time form of $\alpha(\tau)$, when ϕ approaches ϕ_g.

5. Solidification dynamics

In the preceding section we identified a systematic or cooperative mode of movement of particles in which the magnitude and direction of displacement are correlated. This mode has the same statistical manifestation as the symmetry-breaking transverse mode first identified in molecular dynamics simulations of Rahman. We inferred further that when the colloidal fluid is in stable equilibrium this mode dissipates locally. When the volume exceeds the freezing

value the systematic mode remains intact to the upper limit of the experimental time window. In this case the systematic mode comprises a queue of particles in contact. It is plausible that these queues are precursors of the crystal phase.

Crossover times, τ_v and τ_m, and the negative non-Gaussian parameter point to a coupling of the liquid's vorticity to a systematic movement of particles by virtue of a structure that is the same for all volume fractions below the melting value. Therefore, we seek to determine a universal aspect of systematic movement that is compatible with the hydrodynamics of the suspending liquid as well as packing constraints among the particles.

It is also evident from the above that the characteristics of the MSD at delay time, τ_m, play a central role. At this time the MSD can be expressed as

$$\langle \Delta r^2(\tau) \rangle \propto \tau^{\nu}. \tag{19}$$

At τ_m there seems to be a dynamic balance between the collective response of the particles to their packing constraints and the non-steady response of the liquid.

We now introduce a scheme, based on the index ν, that allows our observations on hard-sphere suspensions to be collated and address the above questions about crystallization and the influence of the liquid's vorticity.

There are two values of ν with obvious meaning: $\nu = 1$ indicates random movement, i.e., no queueing; and $\nu = 0$ indicates arrest. An interpretation used to describe fluctuations in other types of complex behaviour points to two further key values of the index ν [24]. One, $\nu = 1/2$, indicates that the variable Δr fluctuates by virtue of random interruption. The other, $\nu = 1/3$, indicates that Δr is subject entirely to anti-correlated interruption. In other words, movement of a queue in a given direction causes a disturbance which, after some delay, forces the queue in the opposite direction.

On the basis of the above characteristic values of ν, it is possible to diagrammatically represent the dynamical response to (osmotic) compression of the suspension by drawing curves, $\nu_j^{(k)}(\phi)$ in the ν–ϕ plane, determined by the dimension, j, of the space to which particle displacements are confined. These curves are subject to the following rules and definitions:

(i) The index ν is an indicator of the efficiency with which configuration space is explored or entropy is gained.

(ii) The quantity $1 - |\nu_j^{(k)} - \nu_i^{(l)}|$ gives a measure of the probability of a transition (or feedback) between curves $\nu_{(i)}^{(l)}(\phi)$ and $\nu_j^{(k)}(\phi)$. Thus, a given curve feeds back positively to one below it and negatively to one above it.

(iii) Where a given curve intercepts the value $1/2$, the mode of exploration of configuration space that it represents is metastable to the nearest curve that lies above it. Where a curve intercepts the value $1/3$, it is unstable. An exception to the last rule will be introduced later.

(iv) A (feedback) loop is stable, or equilibrates, when it reaches or intercepts the value $\nu = 1$.

Consider the curves drawn in the lower half of figure 11. The straight line,

$$\nu_3^{(1)} = \left(1 - \frac{\phi}{\phi_c}\right), \tag{20}$$

between the points ($\phi = 0$, $\nu = 1$) and ($\phi_c = 0.74$, $\nu = 0$) is the line of (tagged particle) density fluctuations in three dimensions. Regular close packing of hard spheres at the volume fraction $\phi_c = 0.74$ is assumed. This simple isotropic dynamical response to compression of the suspension encounters interruptions, $\nu = 1/2$ at $\phi = 0.37$ and $\nu = 1/3$ at $\phi_{fa} = 0.4933$.

A second curve

$$\nu_1^{(1)} = \left(1 - \frac{\phi}{\phi_{ga}}\right)^{1/3} \tag{21}$$

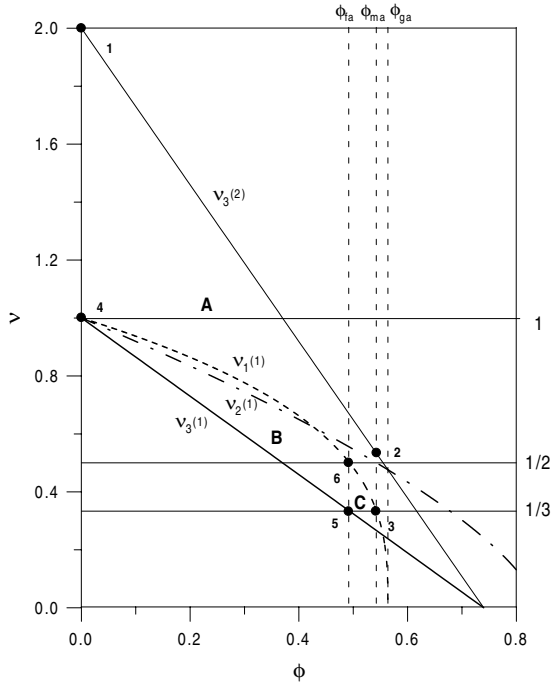

Figure 11. The bold lines indicate the dependence of the index ν on the volume fraction for tagged particle density fluctuations in one, two and three dimensions, respectively expressed by $\nu_1^{(1)}$ (dashed curve, equation (21)), $\nu_2^{(1)}$ (dash–dot curve, equation (22)) and $\nu_3^{(1)}$ (continuous line, equation (20)). The light line is the momentum line $\nu_3^{(2)}$ (equation (23)). Fine horizontal lines are drawn for $\nu = 1/3$, $1/2$ and 1. Dashed vertical lines are drawn successively at $\phi_{fa} = 0.4933$, $\phi_{ma} = 0.5429$ and $\phi_{ga} = 0.5638$. The heavy dots are vertices of loops A, B and C. See the text for an explanation.

restricts displacements to one dimension. Here we assume that the instability of isotropic clusters, at ϕ_{fa}, must be relieved by a transition to movement in a space of lower dimension. Guided by Rahman's computations, we assume that this is achieved by slippage into one dimension. The volume fraction, $\phi_{ga} = 0.5638$, is selected to force equation (21) through the point (ϕ_{fa}, $\nu = 1/2$). As a consequence, the line $\nu_1^{(1)}$ reaches an instability, $\nu = 1/3$, at $\phi_{ma} = 0.5439$.

Having impeded movement in one and three dimensions, the remaining possibility is confinement to planes. This is represented by the curve

$$\nu_2^{(1)} = \left(1 - \frac{\phi}{\phi_X}\right)^{2/3}. \tag{22}$$

When equation (22) is forced through the point $(1/2, \phi_{ma})$ it also passes through the points $(1/3, 0.6782)$ and $(0, \phi_X = 0.8398)$.

Several points of agreement with observation should be noted: the values $\phi_{fa} = 0.4933$ and $\phi_{ma} = 0.5439$ agree with the freezing and melting values based on computer simulation [25] and observed experimentally [6]. Extrapolation of the line $\nu_1^{(1)}$ into the entropically unstable region to $\nu = 0$ gives a GT at $\phi_{ga} = 0.5638$. The experimental GT is located at $\phi_g = 0.575 \pm 0.005$. The proximity of the curve $\nu_1^{(1)}(\phi)$ to the measured index ν (see figure 4) confirms that particle movements confined to one dimension make the dominant contribution to the MSD when observed over the time interval τ_m. The differences between

the experimental values of ν and the location of the GT and those mapped out in figure 11 are small but significant. Below, we address the issue of polydispersity which explains these differences, at least qualitatively.

The structural or entropic instabilities, at the volume fractions $\phi_{fa} = 0.4933$ and $\phi_{ma} = 0.5439$, while symptomatic of freezing and melting, do not in themselves explain how a three-dimensional crystal forms. In fact, formation of three-dimensional structures is impeded at ϕ_{fa}. Furthermore, extrapolation of the line of planes, $\nu_2^{(1)}(\phi)$, leads to unphysical volume fractions.

From this scheme it is apparent that entropy alone is not able to carry the metastable fluid to the equilibrium crystal.

The scheme proposed so far does not account for the coupling between particle movement and the non-steady response of the liquid. To incorporate the latter, figure 11 is augmented with the line representing isotropic momentum fluctuations:

$$\nu_3^{(2)} = 2\left(1 - \frac{\phi}{\phi_c}\right). \tag{23}$$

Statistically, unimpeded ballistic motion is represented by the value, $\nu = 2$, of the index in equation (19). At ϕ_c no motion is possible and $\nu = 0$. We assume that the particles are perfectly buoyant and that the suspending liquid is a continuum. The latter means that the line $\nu_3^{(2)}(\phi)$ is unaffected by packing constraints among the particles and can pass through the values $1/2$ and $1/3$ uninterrupted. This is the exception to rule (iii) anticipated above.

There are numerous possible (feedback) loops. We consider three that have a (lower) vertex on the line, $\nu = 1/3$. The first of these encompasses curves $\nu_3^{(2)}$ and $\nu_1^{(1)}$, and vertices $(\phi = 0, \nu = 2)$, $(\phi_{ma}, \nu_3^{(2)}(\phi_{ma}))$, $(\phi_{ma}, 1/3)$ and $(0, 1)$. This may be read from figure 11 as loop A through points 1, 2, 3 and 4. In this we have a schematic illustration of the positive feedback provided by isotropic momentum fluctuations to the line $\nu_1^{(1)}(\phi)$. Recall that the latter represents systematic particle movement in one dimension and that actual value of ν, along any curve, represents the efficiency of configuration space traversal. Thus, the value of ν along the curve $\nu_1^{(1)}(\phi)$ embodies contributions from concerted and random motion of particles in a file. Only the concerted movement, that for which $\langle \Delta r^2(\tau) \rangle \propto \tau^{1/2}$, benefits from the feedback. The resulting VAF must, therefore, be positive and proportional to $\tau^{-3/2}$.

By rule (iv), loop A is stable. This merely states that momentum fluctuations equilibrate for $\phi < \phi_{ma}$. The results for $P(q, \tau < \tau_m)$, in figure 8(b), indicate that this equilibration is achieved in the interval τ_m.

The second loop encompasses $\nu_1^{(1)}(\phi)$ and $\nu_3^{(1)}(\phi)$, and passes through $(0, 1)$, $(\phi_{fa}, 1/3)$ and $(\phi_{fa}, 1/2)$. This is indicated in figure 11 as loop B through points 4, 5 and 6. By the reasoning used above, isotropic density fluctuations feed into the line $\nu_1^{(1)}(\phi)$. In this case, however, the feedback is negative since the curve $\nu_3^{(1)}(\phi)$ lies below $\nu_1^{(1)}(\phi)$ and, therefore, presents a less efficient traversal of configuration space. Now the VAF is negative and also proportional to $\tau^{-3/2}$.

For the colloidal fluid in stable equilibrium ($\phi < \phi_{fa}$), these loops A and B share the boundary $\nu_1^{(1)}(\phi)$. It is apparent from the results of section 4 that the movement of particles, in response to their packing constraints, conspires with the non-steady response of the liquid in manner that leads, as illustrated by their common boundary at τ_m (figure 11), to the most efficient exploration of configuration space. Thus at τ_m the two feedback mechanisms cancel and, as demonstrated by the data, there is no algebraic persistence of the VAF. As mentioned, for $\tau > \tau_m$ momentum fluctuations are random and these dissipate the queues. Consequently, and in compliance with rule (iv), loop B is stable. At large delay times the ISF and correlation function, $P(q, \tau > \tau_m)$, of the slow fluctuations decay exponentially.

We now turn to the coexistence region, $\phi_{fa} \leqslant \phi \leqslant \phi_{ma}$. As before, we read from the normal exponential decay of $P(q, \tau < \tau_m)$ that, up to ϕ_m, momentum fluctuations are random over the interval τ_m. Thus the boundary $\nu_1^{(1)}(\phi)$ between ϕ_{fa} and ϕ_{ma} is an essential aspect of the dynamics in the coexistence region and, consequently, the dynamics of the particles is determined by the loop (C) with vertices $(1/3, \phi_{fa})$, $(1/2, \phi_{fa})$ and $(1/3, \phi_{ma})$. Loop C (through points 5, 6 and 3) does not intercept the line $\nu = 1$ and, therefore, the unstable isotropic clusters at ϕ_{fa} and unstable files at ϕ_{ma} are unable to equilibrate without transition to the momentum line. Such transitions are random. But they present a process by which entropically unstable structures acquire the binding energy that stabilizes them. The randomness of these stabilizing transitions would also render the colloidal fluid in the coexistence region metastable to crystallization. Furthermore, according to rule (ii) above, a transition from unstable files to the momentum line (point 3 to 2) is more probable than a transition from the unstable clusters (point 5 to the point $\nu_3^{(2)}(\phi_{fa})$). This suggests that, in the coexistence region, crystallization occurs by alignment and registration of files.

Given that loops A and B are stable in the sense that they provide the dynamical route to equilibrium, they cannot be traversed by another line. Therefore the line of planes $\nu_2^{(1)}(\phi)$ is statistically not allowed. However, were this line to 'tunnel' through to the point $(1/2, \phi_{ma})$, its close proximity to the momentum line would render planes only weakly metastable to registration by the momentum.

For higher volume fractions, $\phi > \phi_{ma}$, we have seen from $P(q, \tau < \tau_m)$ that the non-steady motion is no longer random in the interval τ_m. Thus, any structures, files, planes or isotropic structures, that pass beyond ϕ_{ma} are systematically bound by the liquid's vorticity. Consequently, the colloidal fluid with a volume fraction greater than ϕ_{ma} is unstable to crystallization. Note also, in figure 11, that the momentum line intercepts the line $\nu_2^{(1)}(\phi)$ at ϕ_{ga}. This provides another mechanism by which the unphysical extrapolation, $\nu_2^{(1)}(\phi_X = 0.8398) = 0$, is avoided.

By rule (iv) the system is unable to equilibrate in any way when $\phi > \phi_{ma}$. The line $\nu = 1$ is excluded from this region by the momentum line. This simply means that the crystal is infinite in extent and the average over orientations required for equation (1) cannot be fulfilled.

One of the questions about the hard-sphere suspensions is: what makes them so resilient to crystallization at volume fractions ($\phi > \phi_{ma}$) where we have just argued they should be unstable to it?

The discussion so far assumes that the suspended spheres are identical. However, one expects, when there is a (small) distribution of particle radii, that regular configurations will take longer to form and will, therefore, be less probable in three dimensions than in two dimensions. And the latter are less probable than one-dimensional structures. Turning this reasoning around, the relative probabilities of finding regular files, planes and clusters are larger in a polydisperse system than they are in a strictly monodisperse system.

One consequence, seen in figure 4, is that the curve $\nu_1^{(1)}$ is enhanced. Another consequence is that the efficacy of the liquid's vorticity in binding structures in three dimensions is impaired. One expects this, in turn, to enhance the lifetime of the metastable colloidal fluid in the coexistence region and provide it with a degree of (meta)stability at higher volume fractions. A third consequence is that the curve of planes, $\nu_2^{(1)}$, has weighting that it would not have for a monodisperse suspension. Persistence of this curve beyond ϕ_{ma} carries the GT to a volume fraction higher than ϕ_{ga}. This provides a possible qualitative explanation for the difference, noted above, between ϕ_{ga} and the volume fraction, ϕ_g, of the observed GT. It may also explain why we find that colloidal glasses ultimately crystallize and do so by forming large crystals that appear to be seeded by planes [26].

We close by listing a few issues that we hope to address in the future:

(i) There are interruption points and loops in figure 11 not considered above but which warrant explanation.
(ii) The scheme presented in figure 11 is still incomplete. It does not consider the energy source of the fluctuations.
(iii) The above must be augmented by the coherent ISF. This may give the analyses and interpretations the spatial context that they currently lack.
(iv) Description of the key features of the fluctuations, pointed out above, is not possible without consideration of feedback that is non-local in space and time. Mode-coupling theories satisfy this requirement in principle.

Acknowledgments

The basic measurements given and discussed in this paper were done by Tim Mortensen. The results of these measurements will be reported in detail in another publication. I am grateful to Gary Bryant and Salvy Russo for many discussions and their comments on this paper.

References

[1] Paul G L and Pusey P N 1981 *J. Phys. A: Math. Gen.* **14** 3301
[2] Alder B J and Wainwright T E 1970 *Phys. Rev.* A **1** 18
[3] Zwanzig R and Bixon M 1970 *Phys. Rev.* A **2** 2005
[4] Pusey P N 1991 *Liquids, Freezing and the Glass Transition (Les Houches Session L1)* ed D Levesque, J-P Hansen and J Zinn-Justin (Amsterdam: North-Holland) p 763
[5] Kelton K F 1991 *Solid State Physics* ed H Ehrenreich and O Turnbull (New York: Academic) p 75
[6] Pusey P N and van Megen W 1986 *Nature* **320** 340
[7] Pusey P N and van Megen W 1984 *J. Chem. Phys.* **80** 3513
[8] Henderson S I *et al* 1995 *Physica* A **233** 102
Henderson S I and van Megen W 1998 *Phys. Rev. Lett.* **80** 877
[9] Pusey P N and van Megen W 1987 *Phys. Rev. Lett.* **59** 2083
[10] Segrè P N and Pusey P N 1996 *Phys. Rev. Lett.* **77** 771
[11] van Megen W and Underwood S M 1994 *Phys. Rev.* E **49** 4206
[12] Götze W 1999 *J. Phys.: Condens. Matter* **11** A1
[13] Nijboer B R A and Rahman A 1966 *Physica* **32** 415
[14] van Megen W, Mortensen T C, Williams S R and Müller J 1998 *Phys. Rev.* E **58** 6073
[15] Rahman A 1966 *J. Chem. Phys.* **45** 2585
[16] Kegel W and van Blaaderen A 2000 *Science* **287** 290
Weeks E R *et al* 2000 *Science* **287** 627
Glotzer S C 2000 *J. Non-Cryst. Solids* **274** 342
Doliwa B and Heuer A 2000 *Phys. Rev.* E **61** 6898
[17] van Megen W and Mortensen T C 2002 at press
[18] Harris T E 1965 *J. Appl. Probab.* **2** 323
van Beijeren H, Kher K W and Kutner R 1983 *Phys. Rev.* B **28** 5711
[19] Wei Q H, Bechinger C and Leiderer P 2000 *Science* **287** 625
[20] Finney J L 1970 *Proc. R. Soc.* A **319** 479
[21] Götze W and Sjögren L 1991 *Phys. Rev.* A **43** 5442
[22] Williams S R, unpublished
[23] Chandrasekhar S 1943 *Rev. Mod. Phys.* **15** 1
[24] Mantegna R N and Stanley H E 2000 *An Introduction to Econophysics* (Cambridge: Cambridge University Press)
[25] Hoover W G and Ree F H 1968 *J. Chem. Phys.* **49** 3609
[26] van Megen W and Underwood S M 1993 *Nature* **362** 616